

1 **Search for pair-production of strongly-interacting particles**
2 **decaying to pairs of jets in $p\bar{p}$ collisions at $\sqrt{s} = 1.96$ TeV**

3 T. Aaltonen,²¹ E. Albin,⁵⁷ S. Amerio,⁴⁰ D. Amidei,³² A. Anastassov^x,¹⁵ A. Annovi,¹⁷ J. Antos,¹² G. Apollinari,¹⁵
4 J.A. Appel,¹⁵ T. Arisawa,⁵³ A. Artikov,¹³ J. Asaadi,⁴⁸ W. Ashmanskas,¹⁵ B. Auerbach,² A. Aurisano,⁴⁸ F. Azfar,³⁹
5 W. Badgett,¹⁵ T. Bae,²⁵ A. Barbaro-Galtieri,²⁶ V.E. Barnes,⁴⁴ B.A. Barnett,²³ P. Barria^{hh},⁴² P. Bartos,¹²
6 M. Bauc^{ff},⁴⁰ F. Bedeschi,⁴² S. Behari,¹⁵ G. Bellettini^{gg},⁴² J. Bellinger,⁵⁵ D. Benjamin,¹⁴ A. Beretvas,¹⁵
7 A. Bhatti,⁴⁶ K.R. Bland,⁵ B. Blumenfeld,²³ A. Bocci,¹⁴ A. Bodek,⁴⁵ D. Bortoletto,⁴⁴ J. Boudreau,⁴³ A. Boveia,¹¹
8 L. Brigliadori^{ee},⁶ C. Bromberg,³³ E. Brucken,²¹ J. Budagov,¹³ H.S. Budd,⁴⁵ K. Burkett,¹⁵ G. Busetto^{ff},⁴⁰
9 P. Bussey,¹⁹ P. Butti^{gg},⁴² A. Buzatu,¹⁹ A. Calamba,¹⁰ S. Camarda,⁴ M. Campanelli,²⁸ F. Canelli^{oo},^{11,15}
10 B. Carls,²² D. Carlsmith,⁵⁵ R. Carosi,⁴² S. Carrillo^m,¹⁶ B. Casal^k,⁹ M. Casarsa,⁴⁹ A. Castro^{ee},⁶ P. Catastini,²⁰
11 D. Cauz,⁴⁹ V. Cavaliere,²² M. Cavalli-Sforza,⁴ A. Cerri^f,²⁶ L. Cerrito^s,²⁸ Y.C. Chen,¹ M. Chertok,⁷ G. Chiarelli,⁴²
12 G. Chlachidze,¹⁵ K. Cho,²⁵ D. Chokheli,¹³ M.A. Ciocci^{hh},⁴² A. Clark,¹⁸ C. Clarke,⁵⁴ M.E. Convery,¹⁵ J. Conway,⁷
13 M. Corbo,¹⁵ M. Cordelli,¹⁷ C.A. Cox,⁷ D.J. Cox,⁷ M. Cremonesi,⁴² D. Cruz,⁴⁸ J. Cuevas^z,⁹ R. Culbertson,¹⁵
14 N. d'Ascenzo^w,¹⁵ M. Datta^{qq},¹⁵ P. De Barbaro,⁴⁵ L. Demortier,⁴⁶ M. Deninno,⁶ F. Devoto,²¹ M. d'Errico^{ff},⁴⁰
15 A. Di Canto^{gg},⁴² B. Di Ruzza^q,¹⁵ J.R. Dittmann,⁵ M. D'Onofrio,²⁷ S. Donati^{gg},⁴² M. Dorigoⁿⁿ,⁴⁹ A. Driutti,⁴⁹
16 K. Ebina,⁵³ R. Edgar,³² A. Elagin,⁴⁸ R. Erbacher,⁷ S. Errede,²² B. Esham,²² R. Eusebi,⁴⁸ S. Farrington,³⁹
17 J.P. Fernández Ramos,²⁹ R. Field,¹⁶ G. Flanagan^u,¹⁵ R. Forrest,⁷ M. Franklin,²⁰ J.C. Freeman,¹⁵ H. Frisch,¹¹
18 Y. Funakoshi,⁵³ A.F. Garfinkel,⁴⁴ P. Garosi^{hh},⁴² H. Gerberich,²² E. Gerchtein,¹⁵ S. Giagu,⁴⁷ V. Giakoumopoulou,³
19 K. Gibson,⁴³ C.M. Ginsburg,¹⁵ N. Giokaris,³ P. Giromini,¹⁷ G. Giurgiu,²³ V. Glagolev,¹³ D. Glenzinski,¹⁵
20 M. Gold,³⁵ D. Goldin,⁴⁸ A. Golossanov,¹⁵ G. Gomez,⁹ G. Gomez-Ceballos,³⁰ M. Goncharov,³⁰ O. González López,²⁹
21 I. Gorelov,³⁵ A.T. Goshaw,¹⁴ K. Goulianos,⁴⁶ E. Gramellini,⁶ S. Grinstein,⁴ C. Grosso-Pilcher,¹¹ R.C. Group^{52,15},
22 J. Guimaraes da Costa,²⁰ S.R. Hahn,¹⁵ J.Y. Han,⁴⁵ F. Happacher,¹⁷ K. Hara,⁵⁰ M. Hare,⁵¹ R.F. Harr,⁵⁴
23 T. Harrington-Taberⁿ,¹⁵ K. Hatakeyama,⁵ C. Hays,³⁹ J. Heinrich,⁴¹ M. Herndon,⁵⁵ A. Hocker,¹⁵ Z. Hong,⁴⁸
24 W. Hopkins^g,¹⁵ S. Hou,¹ R.E. Hughes,³⁶ U. Husemann,⁵⁶ M. Hussein,³³ J. Huston,³³ G. Introzzi^{mm},⁴² M. Iori^{jj},⁴⁷
25 A. Ivanov^p,⁷ E. James,¹⁵ D. Jang,¹⁰ B. Jayatilaka,¹⁵ E.J. Jeon,²⁵ S. Jindariani,¹⁵ M. Jones,⁴⁴ K.K. Joo,²⁵
26 S.Y. Jun,¹⁰ T.R. Junk,¹⁵ M. Kambeitz,²⁴ T. Kamon^{25,48}, P.E. Karchin,⁵⁴ A. Kasmi,⁵ Y. Kato^o,³⁸ W. Ketchum^{rr},¹¹
27 J. Keung,⁴¹ B. Kilminster^{oo},¹⁵ D.H. Kim,²⁵ H.S. Kim,²⁵ J.E. Kim,²⁵ M.J. Kim,¹⁷ S.B. Kim,²⁵ S.H. Kim,⁵⁰
28 Y.K. Kim,¹¹ Y.J. Kim,²⁵ N. Kimura,⁵³ M. Kirby,¹⁵ K. Knoepfel,¹⁵ K. Kondo^{*},⁵³ D.J. Kong,²⁵ J. Konigsberg,¹⁶
29 A.V. Kotwal,¹⁴ M. Kreps,²⁴ J. Kroll,⁴¹ M. Kruse,¹⁴ T. Kuhr,²⁴ M. Kurata,⁵⁰ A.T. Laasanen,⁴⁴ S. Lammel,¹⁵
30 M. Lancaster,²⁸ K. Lannon^y,³⁶ G. Latino^{hh},⁴² H.S. Lee,²⁵ J.S. Lee,²⁵ S. Leo,⁴² S. Leone,⁴² J.D. Lewis,¹⁵
31 A. Limosani^t,¹⁴ E. Lipeles,⁴¹ H. Liu,⁵² Q. Liu,⁴⁴ T. Liu,¹⁵ S. Lockwitz,⁵⁶ A. Loginov,⁵⁶ D. Lucchesi^{ff},⁴⁰
32 J. Lueck,²⁴ P. Lujan,²⁶ P. Lukens,¹⁵ G. Lungu,⁴⁶ J. Lys,²⁶ R. Lysak^e,¹² R. Madrak,¹⁵ P. Maestro^{hh},⁴² S. Malik,⁴⁶
33 G. Manca^a,²⁷ A. Manousakis-Katsikakis,³ F. Margaroli,⁴⁷ P. Marinoⁱⁱ,⁴² M. Martínez,⁴ K. Matera,²²
34 M.E. Mattson,⁵⁴ A. Mazzacane,¹⁵ P. Mazzanti,⁶ R. McNulty^j,²⁷ A. Mehta,²⁷ P. Mehtala,²¹ C. Mesropian,⁴⁶
35 T. Miao,¹⁵ D. Mietlicki,³² A. Mitra,¹ H. Miyake,⁵⁰ S. Moed,¹⁵ N. Moggi,⁶ C.S. Moon^{aa},¹⁵ R. Moore^{pp},¹⁵
36 M.J. Morelloⁱⁱ,⁴² A. Mukherjee,¹⁵ Th. Muller,²⁴ P. Murat,¹⁵ M. Mussini^{ee},⁶ J. Nachtmanⁿ,¹⁵ Y. Nagai,⁵⁰
37 J. Naganoma,⁵³ I. Nakano,³⁷ A. Napier,⁵¹ J. Nett,⁴⁸ C. Neu,⁵² T. Nigmanov,⁴³ L. Nodulman,² S.Y. Noh,²⁵
38 O. Norniella,²² L. Oakes,³⁹ S.H. Oh,¹⁴ Y.D. Oh,²⁵ I. Oksuzian,⁵² T. Okusawa,³⁸ R. Orava,²¹ L. Ortolan,⁴
39 C. Pagliarone,⁴⁹ E. Palencia^f,⁹ P. Palni,³⁵ V. Papadimitriou,¹⁵ W. Parker,⁵⁵ G. Pauletta^{kk},⁴⁹ M. Paulini,¹⁰
40 C. Paus,³⁰ T.J. Phillips,¹⁴ G. Piacentino,⁴² E. Pianori,⁴¹ J. Pilot,³⁶ K. Pitts,²² C. Plager,⁸ L. Pondrom,⁵⁵
41 S. Poprocki^g,¹⁵ K. Potamianos,²⁶ F. Prokoshin^{cc},¹³ A. Pranko,²⁶ F. Ptohos^h,¹⁷ G. Punzi^{gg},⁴² N. Ranjan,⁴⁴
42 I. Redondo Fernández,²⁹ P. Renton,³⁹ M. Rescigno,⁴⁷ T. Riddick,²⁸ F. Rimondi^{*},⁶ L. Ristori^{42,15}, A. Robson,¹⁹
43 T. Rodriguez,⁴¹ S. Rolliⁱ,⁵¹ M. Ronzani^{gg},⁴² R. Roser,¹⁵ J.L. Rosner,¹¹ F. Ruffini^{hh},⁴² A. Ruiz,⁹ J. Russ,¹⁰
44 V. Rusu,¹⁵ A. Safonov,⁴⁸ W.K. Sakumoto,⁴⁵ Y. Sakurai,⁵³ L. Santi^{kk},⁴⁹ K. Sato,⁵⁰ V. Saveliev^w,¹⁵
45 A. Savoy-Navarro^{aa},¹⁵ P. Schlabach,¹⁵ E.E. Schmidt,¹⁵ T. Schwarz,³² L. Scodellaro,⁹ F. Scuri,⁴² S. Seidel,³⁵
46 Y. Seiya,³⁸ A. Semenov,¹³ F. Sforza^{gg},⁴² S.Z. Shalhout,⁷ T. Shears,²⁷ P.F. Shepard,⁴³ M. Shimojima^v,⁵⁰
47 M. Shochet,¹¹ I. Shreyber-Tecker,³⁴ A. Simonenko,¹³ P. Sinervo,³¹ K. Sliwa,⁵¹ J.R. Smith,⁷ F.D. Snider,¹⁵ V. Sorin,⁴
48 H. Song,⁴³ M. Stancari,¹⁵ R. St. Denis,¹⁹ B. Stelzer,³¹ O. Stelzer-Chilton,³¹ D. Stentz^x,¹⁵ J. Strologas,³⁵ Y. Sudo,⁵⁰
49 A. Sukhanov,¹⁵ I. Suslov,¹³ K. Takemasa,⁵⁰ Y. Takeuchi,⁵⁰ J. Tang,¹¹ M. Tecchio,³² P.K. Teng,¹ J. Thom^g,¹⁵

1 E. Thomson,⁴¹ V. Thukral,⁴⁸ D. Toback,⁴⁸ S. Tokar,¹² K. Tollefson,³³ T. Tomura,⁵⁰ D. Tonelli,^{f,15} S. Torre,¹⁷
 2 D. Torretta,¹⁵ P. Totaro,⁴⁰ M. Trovato,^{ii,42} F. Ukegawa,⁵⁰ S. Uozumi,²⁵ F. Vázquez,^{m,16} G. Velev,¹⁵ C. Vellidis,¹⁵
 3 C. Vernieri,^{ii,42} M. Vidal,⁴⁴ R. Vilar,⁹ J. Vizán,^{ii,9} M. Vogel,³⁵ G. Volpi,¹⁷ P. Wagner,⁴¹ R. Wallny,⁸ S.M. Wang,¹
 4 A. Warburton,³¹ D. Waters,²⁸ W.C. Wester III,¹⁵ D. Whiteson,^{b,41} A.B. Wicklund,² S. Wilbur,¹¹ H.H. Williams,⁴¹
 5 J.S. Wilson,³² P. Wilson,¹⁵ B.L. Winer,³⁶ P. Wittich,^{g,15} S. Wolbers,¹⁵ H. Wolfe,³⁶ T. Wright,³² X. Wu,¹⁸ Z. Wu,⁵
 6 K. Yamamoto,³⁸ D. Yamato,³⁸ T. Yang,¹⁵ U.K. Yang,^{r,11} Y.C. Yang,²⁵ W.-M. Yao,²⁶ G.P. Yeh,¹⁵ K. Yi,^{n,15}
 7 J. Yoh,¹⁵ K. Yorita,⁵³ T. Yoshida,^{l,38} G.B. Yu,¹⁴ I. Yu,²⁵ A.M. Zanetti,⁴⁹ Y. Zeng,¹⁴ C. Zhou,¹⁴ and S. Zucchelli^{ee6}

(CDF Collaboration[†])

¹*Institute of Physics, Academia Sinica, Taipei, Taiwan 11529, Republic of China*

²*Argonne National Laboratory, Argonne, Illinois 60439, USA*

³*University of Athens, 157 71 Athens, Greece*

⁴*Institut de Física d'Altes Energies, ICREA, Universitat Autònoma de Barcelona, E-08193, Bellaterra (Barcelona), Spain*

⁵*Baylor University, Waco, Texas 76798, USA*

⁶*Istituto Nazionale di Fisica Nucleare Bologna, ^{ee}University of Bologna, I-40127 Bologna, Italy*

⁷*University of California, Davis, Davis, California 95616, USA*

⁸*University of California, Los Angeles, Los Angeles, California 90024, USA*

⁹*Instituto de Física de Cantabria, CSIC-University of Cantabria, 39005 Santander, Spain*

¹⁰*Carnegie Mellon University, Pittsburgh, Pennsylvania 15213, USA*

¹¹*Enrico Fermi Institute, University of Chicago, Chicago, Illinois 60637, USA*

¹²*Comenius University, 842 48 Bratislava, Slovakia; Institute of Experimental Physics, 040 01 Kosice, Slovakia*

¹³*Joint Institute for Nuclear Research, RU-141980 Dubna, Russia*

¹⁴*Duke University, Durham, North Carolina 27708, USA*

¹⁵*Fermi National Accelerator Laboratory, Batavia, Illinois 60510, USA*

¹⁶*University of Florida, Gainesville, Florida 32611, USA*

¹⁷*Laboratori Nazionali di Frascati, Istituto Nazionale di Fisica Nucleare, I-00044 Frascati, Italy*

¹⁸*University of Geneva, CH-1211 Geneva 4, Switzerland*

¹⁹*Glasgow University, Glasgow G12 8QQ, United Kingdom*

²⁰*Harvard University, Cambridge, Massachusetts 02138, USA*

²¹*Division of High Energy Physics, Department of Physics,*

University of Helsinki and Helsinki Institute of Physics, FIN-00014, Helsinki, Finland

²²*University of Illinois, Urbana, Illinois 61801, USA*

²³*The Johns Hopkins University, Baltimore, Maryland 21218, USA*

²⁴*Institut für Experimentelle Kernphysik, Karlsruhe Institute of Technology, D-76131 Karlsruhe, Germany*

²⁵*Center for High Energy Physics: Kyungpook National University,*

Daegu 702-701, Korea; Seoul National University, Seoul 151-742,

Korea; Sungkyunkwan University, Suwon 440-746,

Korea; Korea Institute of Science and Technology Information,

Daejeon 305-806, Korea; Chonnam National University,

Gwangju 500-757, Korea; Chonbuk National University, Jeonju 561-756,

Korea; Ewha Womans University, Seoul, 120-750, Korea

²⁶*Ernest Orlando Lawrence Berkeley National Laboratory, Berkeley, California 94720, USA*

²⁷*University of Liverpool, Liverpool L69 7ZE, United Kingdom*

²⁸*University College London, London WC1E 6BT, United Kingdom*

²⁹*Centro de Investigaciones Energeticas Medioambientales y Tecnológicas, E-28040 Madrid, Spain*

³⁰*Massachusetts Institute of Technology, Cambridge, Massachusetts 02139, USA*

³¹*Institute of Particle Physics: McGill University, Montréal, Québec H3A 2T8,*

Canada; Simon Fraser University, Burnaby, British Columbia V5A 1S6,

Canada; University of Toronto, Toronto, Ontario M5S 1A7,

Canada; and TRIUMF, Vancouver, British Columbia V6T 2A3, Canada

³²*University of Michigan, Ann Arbor, Michigan 48109, USA*

³³*Michigan State University, East Lansing, Michigan 48824, USA*

³⁴*Institution for Theoretical and Experimental Physics, ITEP, Moscow 117259, Russia*

³⁵*University of New Mexico, Albuquerque, New Mexico 87131, USA*

³⁶*The Ohio State University, Columbus, Ohio 43210, USA*

³⁷*Okayama University, Okayama 700-8530, Japan*

³⁸*Osaka City University, Osaka 588, Japan*

³⁹*University of Oxford, Oxford OX1 3RH, United Kingdom*

⁴⁰*Istituto Nazionale di Fisica Nucleare, Sezione di Padova-Trento, ^{ff}University of Padova, I-35131 Padova, Italy*

⁴¹*University of Pennsylvania, Philadelphia, Pennsylvania 19104, USA*

⁴²*Istituto Nazionale di Fisica Nucleare Pisa*, ⁹⁹*University of Pisa*,
^{hh}*University of Siena* and ⁱⁱ*Scuola Normale Superiore, I-56127 Pisa*,
Italy, ^{mm}*INFN Pavia and University of Pavia, I-27100 Pavia, Italy*

⁴³*University of Pittsburgh, Pittsburgh, Pennsylvania 15260, USA*

⁴⁴*Purdue University, West Lafayette, Indiana 47907, USA*

⁴⁵*University of Rochester, Rochester, New York 14627, USA*

⁴⁶*The Rockefeller University, New York, New York 10065, USA*

⁴⁷*Istituto Nazionale di Fisica Nucleare, Sezione di Roma 1*,

^{jj}*Sapienza Università di Roma, I-00185 Roma, Italy*

⁴⁸*Texas A&M University, College Station, Texas 77843, USA*

⁴⁹*Istituto Nazionale di Fisica Nucleare Trieste/Udine; ⁿⁿUniversity of Trieste*,
I-34127 Trieste, Italy; ^{kk}*University of Udine, I-33100 Udine, Italy*

⁵⁰*University of Tsukuba, Tsukuba, Ibaraki 305, Japan*

⁵¹*Tufts University, Medford, Massachusetts 02155, USA*

⁵²*University of Virginia, Charlottesville, Virginia 22906, USA*

⁵³*Waseda University, Tokyo 169, Japan*

⁵⁴*Wayne State University, Detroit, Michigan 48201, USA*

⁵⁵*University of Wisconsin, Madison, Wisconsin 53706, USA*

⁵⁶*Yale University, New Haven, Connecticut 06520, USA*

⁵⁷*University of California Irvine, Irvine, CA 92697, USA*

We present a search for the pair-production of a non-standard-model strongly-interacting particle that decays to a pair of quarks or gluons, leading to a final state with four hadronic jets. We consider both non-resonant production via an intermediate gluon as well as resonant production via a distinct non-standard-model intermediate strongly-interacting particle. We use data collected by the CDF experiment in proton-antiproton collisions at $\sqrt{s} = 1.96$ TeV corresponding to an integrated luminosity of 6.6 fb^{-1} . We find the data to be consistent with standard model predictions. We report limits on $\sigma(p\bar{p} \rightarrow jjjj)$ as a function of the masses of the hypothetical intermediate particles. Upper limits on the production cross sections for non-standard-model particles in several resonant and non-resonant processes are also derived.

PACS numbers:

One of the few hints of possible physics beyond the standard model (SM) at the TeV scale is the anomalous top-quark forward-backward asymmetry A_{fb} observed at the Tevatron [1–3]. This asymmetry could be generated by non-SM physics through the production of top-quark pairs via a light axi-gluon [4], a particle with axial couplings to quarks, that interferes with standard model (SM) $t\bar{t}$ production to produce the observed asymmetry. The axi-gluon would be visible in its alternate decay mode to low-mass strongly-interacting particles, each of which decays to a pair of jets [5] yielding a four-jet final state. This final state is of broad interest, as various models predict pair-production of strongly-interacting particles decaying to jet pairs with no intermediate resonance [6, 7] and R -parity-violating supersymmetric theories [8] predict pair-production of light partners of the top quark (stop quarks), each decaying into to pairs of light quarks.

The masses of the axi-gluon and its strongly-interacting decay products are not predicted, but must be fairly light ($< 400 \text{ GeV}/c^2$) to explain the A_{fb} measurement [9]. The LHC experiments have excellent sensitivity at high mass due to the large center-of-mass energy, but difficulties at low mass due to high background rates. The ATLAS experiment ruled out masses between 100 and 150 GeV/c^2 [10]. No experimental bounds exist for such non-SM particles with masses below 100 GeV/c^2 for

*Deceased

[†]With visitors from ^a*Istituto Nazionale di Fisica Nucleare, Sezione di Cagliari, 09042 Monserrato (Cagliari), Italy*, ^b*University of California Irvine, Irvine, CA 92697, USA*, ^c*Institute of Physics, Academy of Sciences of the Czech Republic, 182 21, Czech Republic*, ^f*CERN, CH-1211 Geneva, Switzerland*, ^g*Cornell University, Ithaca, NY 14853, USA*, ^h*University of Cyprus, Nicosia CY-1678, Cyprus*, ⁱ*Office of Science, U.S. Department of Energy, Washington, DC 20585, USA*, ^j*University College Dublin, Dublin 4, Ireland*, ^k*ETH, 8092 Zürich, Switzerland*, ^l*University of Fukui, Fukui City, Fukui Prefecture, Japan 910-0017*, ^m*Universidad Iberoamericana, Lomas de Santa Fe, México, C.P. 01219, Distrito Federal*, ⁿ*University of Iowa, Iowa City, IA 52242, USA*, ^o*Kinki University, Higashi-Osaka City, Japan 577-8502*, ^p*Kansas State University, Manhattan, KS 66506, USA*, ^q*Brookhaven National Laboratory, Upton, NY 11973, USA*, ^r*University of Manchester, Manchester M13 9PL, United Kingdom*, ^s*Queen Mary, University of London, London, E1 4NS, United Kingdom*, ^t*University of Melbourne, Victoria 3010, Australia*, ^u*Muons, Inc., Batavia, IL 60510, USA*, ^v*Nagasaki Institute of Applied Science, Nagasaki 851-0193, Japan*, ^w*National Research Nuclear University, Moscow 115409, Russia*, ^x*Northwestern University, Evanston, IL 60208, USA*, ^y*University of Notre Dame, Notre Dame, IN 46556, USA*, ^z*Universidad de Oviedo, E-33007 Oviedo, Spain*, ^{aa}*CNRS-IN2P3, Paris, F-75205 France*, ^{cc}*Universidad Tecnica Federico Santa Maria, 110v Valparaiso, Chile*, ^{dd}*Yarmouk University, Irbid 211-63, Jordan*, ^{ll}*Universite catholique de Louvain, 1348 Louvain-La-Neuve, Belgium*, ^{oo}*University of Zürich, 8006 Zürich, Switzerland*, ^{pp}*Massachusetts General Hospital and Harvard Medical School, Boston, MA 02114 USA*, ^{qq}*Hampton University, Hampton, VA 23668, USA*, ^{rr}*Los Alamos National Laboratory, Los Alamos, NM*

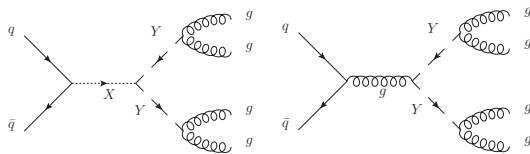


FIG. 1: Diagrams for resonant (left, via X) and non-resonant (right) pair-production of Y particles, with subsequent decays to pairs of gluons. Other models, with final-state quarks, are also considered.

1 non-resonant pair-production of di-jet resonances; there
2 are no current limits on resonant production.

3 In this Letter we report a search for both non-resonant
4 and resonant production of pairs of strongly-interacting
5 particles, each of which decays to a pair of jets. Rather
6 than probing a specific theory, we construct a simplified
7 model with the minimal particle content. In the non-
8 resonant case, we consider the production process $p\bar{p} \rightarrow$
9 $YY \rightarrow jj\,jj$, with the mass of the hypothetical Y state,
10 m_Y as a single free parameter. In the resonant case,
11 $p\bar{p} \rightarrow X \rightarrow YY \rightarrow jj\,jj$, we also explore the mass of the
12 X state, m_X (Fig. 1). In both cases, we assume that the
13 natural width of the particles is small compared to the
14 experimental resolution.

15 We analyze a sample of events corresponding to an in-
16 tegrated luminosity of $6.6 \pm 0.5 \text{ fb}^{-1}$ recorded by the CDF
17 II detector [11], a general purpose detector designed to
18 study $p\bar{p}$ collisions at $\sqrt{s} = 1.96 \text{ TeV}$ produced by the
19 Fermilab Tevatron collider. The tracking system consists
20 of a silicon microstrip tracker and a drift chamber im-
21 mersed in a 1.4 T axial magnetic field [12]. Electromag-
22 netic and hadronic calorimeters surrounding the tracking
23 system measure particle energies, with muon detection
24 provided by an additional system of drift chambers lo-
25 cated outside the calorimeters.

26 We reconstruct jets in the calorimeter using the JET-
27 CLU [13] algorithm with a clustering radius of 0.4 in $\eta - \phi$
28 space [14], and calibrated using the techniques outlined
29 in Ref. [15]. Events are selected online (triggered) by the
30 requirement of three jets, each with $E_T > 20 \text{ GeV}$ and
31 with $\Sigma_{\text{jets}} E_T > 130 \text{ GeV}$ [14]. The data set used in this
32 search is limited to 6.6 fb^{-1} because the trigger selection
33 was not available in early data. After trigger selection,
34 events are retained if at least four jets are found with
35 $E_T > 15 \text{ GeV}$ and $|\eta| < 2.4$.

36 We model resonant and non-resonant production with
37 MADGRAPH5 [16] version 1.4.8.4 and the CTEQ6L1 [17]
38 parton distribution functions (PDF). Additional parton
39 radiation, hadronization, and underlying-event modeling
40 are described by PYTHIA [18] version 6.420. The detec-
41 tor response for all simulated samples is modeled by the
42 GEANT-based CDF II detector simulation [19].

43 The trigger and selection requirements have an effi-
44 ciency on the signal up to 90% if $\Sigma_{\text{jets}} E_T$ exceeds signif-

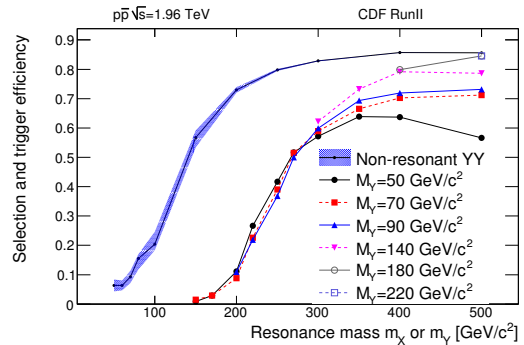


FIG. 2: Overall efficiency, including trigger and selection requirements. Efficiency is shown for several simulated non-resonant $YY \rightarrow jj\,jj$ samples with varying m_Y . The shaded band shows the uncertainty. In addition, efficiency is shown for several simulated resonant $X \rightarrow YY \rightarrow jj\,jj$ samples with varying m_X and m_Y . The uncertainty is not shown but is similar to the non-resonant case. The turn-on curve is determined largely by the trigger requirement that $\Sigma_{\text{jets}} E_T > 130 \text{ GeV}$.

icantly the 130 GeV trigger threshold. For events with
smaller $\Sigma_{\text{jets}} E_T$, the efficiency decreases rapidly (Fig. 2).
In the non-resonant-production model, the $\Sigma_{\text{jets}} E_T$ is
strongly correlated with m_Y . In the resonant-production
model it is correlated with m_X ; additionally if $m_X - 2m_Y$
is large, the p_T of the resulting Y is large, which leads
to a small opening angle of its decay products and a loss
of efficiency due to merged jets. The trigger efficiency is
measured in simulated events, and uncertainties derived
from validation in disjoint samples; the measured trig-
ger efficiency and uncertainty are applied to the signal
model.

To reconstruct the di-jet resonance, we consider the
four leading jets and evaluate the invariant mass of each
of the di-jet pairs in the three permutations, choosing
the permutation with the smallest mass difference be-
tween the pairs. As the pair masses are correlated, we
take the mean of the two pair masses as the estimate of
the di-jet resonance mass. To reduce backgrounds, we
require that the relative mass difference between the two
pairs is less than 50%, and that the production angle
 θ^* of the di-jet resonance in the YY pair center-of-mass
frame satisfies $\cos(\theta^*) < 0.9$. In the resonant production
analysis, we calculate the four-jet invariant mass. No spe-
cific m_Y -dependent selections are made; the requirement
that the relative di-jet mass difference be small ensures
compatibility with the $X \rightarrow YY$ hypothesis. Figures 3
and 4 show the observed di-jet and four-jet spectra, re-
spectively.

The dominant background originates from standard
QCD multi-jet production. We model this background
contribution using a parametric function which is fit to
the reconstructed mass spectrum of the observed data.
The function is a piece-wise combination of a third-order

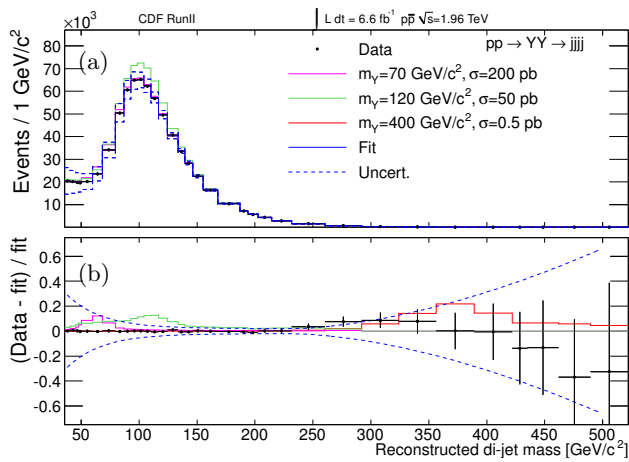


FIG. 3: Reconstructed mean di-jet mass in events with four jets. Parametric fit and several signal hypotheses overlaid in (a). Relative difference between the observed data and the fit in each bin shown in (b).

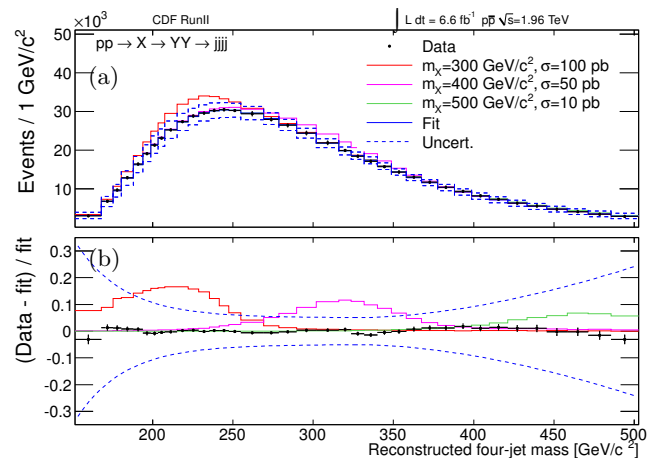


FIG. 4: Reconstructed four-jet mass in events with four jets. Parametric fit and several signal hypotheses overlaid in (a). Relative difference between the observed data and the fit in each bin shown in (b).

1 polynomial to describe the turn-on region, a third-order 36
 2 polynomial to describe the peak region, and a double ex- 37
 3 ponential of the form $f(m) = a_1 e^{-(m-a_2)^{a_3}/a_4}$ to describe 38
 4 the falling spectrum. The parametric functional form 39
 5 was chosen to be flexible enough to describe the multi- 40
 6 jet mass spectrum, but rigid enough to avoid accurately 41
 7 describing a spectrum which includes a narrow resonance, 42
 8 so that in the presence of a narrow feature a signal-plus-
 9 background hypothesis would be preferred. For the di-
 10 jet mass, the ranges used are $[35, 82.5]$, $[82.5, 140]$, and
 11 $[140, 700]$ GeV/c^2 ; for the four-jet mass, the ranges used
 12 are $[115, 185]$, $[185, 330]$, and $[330, 800]$ GeV/c^2 . The
 13 functional form and ranges were chosen based on their
 14 ability to accurately describe the mass spectra of simu-
 15 lated multi-jet events generated by ALPGEN [20] version
 16 2.10.

17 The dominant source of systematic uncertainty is due 43
 18 to the multi-jet background model. The functional form 44
 19 is an approximation, which even in the absence of a nar- 45
 20 row feature may deviate from the observed spectrum. 46
 21 We estimate the impact of these potential deviations by 47
 22 measuring their magnitude in two background-enriched 48
 23 control samples. These two control samples are adjacent 49
 24 to the signal region and capture the expected deviations 50
 25 in two independent directions. The first requires a large 51
 26 relative di-jet mass difference, greater than 50%, and the 52
 27 second requires $\cos(\theta^*) > 0.9$. The observed relative de- 53
 28 viations are then applied to the observed spectrum in 54
 29 the signal region to estimate the magnitude of spurious 55
 30 deviations due to possible mismodeling. In addition, we 56
 31 verify that the fitting procedure gives an unbiased esti- 57
 32 mate of the signal rate. 58

33 An additional uncertainty is due to knowledge of the 59
 34 trigger efficiency [21] extracted from the simulated sig- 60
 35 nal samples, varying from 20% relative at $\Sigma_{\text{jets}} E_T = 120$ 61

GeV to 10% above $\Sigma_{\text{jets}} E_T = 200$ GeV. Uncertainties
 in the levels of parton radiation [22] and in the calibra-
 tion of the jet energy and resolution modeling [15] also
 contribute to uncertainties in the trigger and selection
 efficiency and reconstructed mass spectrum of the signal
 samples. These uncertainties are small ($< 10\%$) relative
 to the fitting and trigger uncertainties.

In the non-resonant analysis, for each Y mass hypoth-
 esis, we fit the most likely value of the Y pair-produc-
 tion cross section (σ_{YY}) by performing a maximum likelihood
 fit of the binned di-jet mass distribution, allowing for sys-
 tematic and statistical fluctuations via template morph-
 ing [23]. The likelihood takes the form of

$$L(\sigma_{YY}) = \prod_{\text{bin } i} f_{\text{bg}}^i(\vec{a}) + \sigma_{YY} \mathcal{L} \in f_{\text{sig}},$$

where $f_{\text{bg}}(\vec{a})$ is the parametric function with nuisance
 parameters \vec{a} defined above to describe the background
 spectrum, f_{sig} is a normalized template of the expected
 shape of the signal determined from simulated events,
 and $\mathcal{L} \in$ is the product of the integrated luminosity and
 efficiency. No evidence is found for the presence of pair-
 production of di-jet resonances and upper limits on Y
 pair-production at 95% confidence level (C.L.) are set.

Limits are calculated using the CLs [24] method by
 repeating the measurement on sets of simulated exper-
 iments that include signal contributions corresponding
 to various hypothetical production cross-sections, and
 variation of systematic uncertainties. The values of nu-
 sance parameters are not fit in the experiments. The
 observed limits are consistent with expectation for the
 background-only hypothesis. The resonant analysis is
 very similar, but is done as a function of the X mass
 hypothesis, fitting the four-jet mass distribution for the
 most likely value of X production cross section, σ_X .

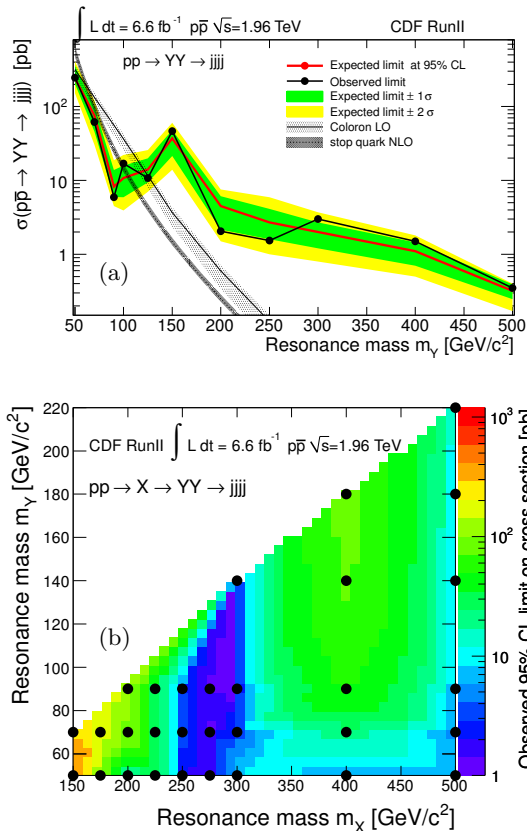


FIG. 5: Upper limit on signal production rate at 95% C.L. Expected and observed upper limits on $\sigma(pp \rightarrow YY \rightarrow jjjj)$ versus m_Y in the non-resonant analysis shown in (a). Two signal hypotheses are shown, see text for details. Observed limits on $\sigma(pp \rightarrow X \rightarrow YY \rightarrow jjjj)$ versus m_X and m_Y shown in (b). Circles indicate the true values of the parameters used in each ensemble of simulated samples used to evaluate the limits; intermediate values are interpolated.

TABLE I: Observed and expected 95% C.L. upper limits on $\sigma(pp \rightarrow YY \rightarrow jj jj)$ for several values of m_Y . Also shown are theoretical predictions for coloron pair production [6, 7] or stop-quark pair production with R -parity-violating decay $\tilde{t} \rightarrow qq'$ [26].

| Mass (GeV/c^2) | Expected (pb) | Observed (pb) | Coloron (pb) | Stop quarks (pb) |
|------------------------------|------------------|------------------|----------------------|----------------------|
| 50 | 240 | 250 | 320 | 570 |
| 70 | 75 | 62 | 180 | 100 |
| 90 | 8.2 | 5.9 | 62 | 26 |
| 100 | 11 | 17 | 37 | 15 |
| 125 | 14 | 11 | 11 | 4.4 |
| 150 | 37 | 46 | 3.7 | 1.5 |
| 200 | 4.5 | 2.0 | 0.60 | 0.25 |
| 250 | 2.7 | 1.5 | 0.11 | 5.4×10^{-2} |
| 300 | 2.0 | 3.0 | 2.9×10^{-2} | 1.3×10^{-2} |
| 400 | 1.1 | 1.5 | 1.7×10^{-3} | 7.2×10^{-4} |
| 500 | 0.3 | 0.3 | 8.5×10^{-5} | 3.6×10^{-5} |

TABLE II: Observed and expected 95% C.L. upper limits on $\sigma(pp \rightarrow X \rightarrow YY \rightarrow jj jj)$ for several values of m_Y and m_X . Also shown are theoretical predictions for axi-gluon production assuming coupling to quarks of $C_q = 0.4$ [5, 9].

| m_X (GeV/c^2) | m_Y (GeV/c^2) | Expected (pb) | Observed (pb) | Axi-gluon (pb) |
|-------------------------------|-------------------------------|------------------|------------------|-------------------|
| 150 | 50 | 641.2 | 431.1 | 5600 |
| | 70 | 209.6 | 270.6 | |
| 175 | 50 | 66.8 | 78.9 | 3500 |
| | 70 | 111.5 | 163.9 | |
| 200 | 50 | 13.8 | 9.5 | 2200 |
| | 70 | 30.4 | 91.5 | |
| | 90 | 17.8 | 100.4 | |
| 225 | 50 | 18.0 | 26.0 | 1750 |
| | 70 | 20.7 | 25.0 | |
| | 90 | 20.9 | 25.3 | |
| 250 | 50 | 6.2 | 2.0 | 1000 |
| | 70 | 4.0 | 3.6 | |
| | 90 | 5.1 | 2.8 | |
| 275 | 50 | 6.5 | 1.2 | 850 |
| | 70 | 7.7 | 1.3 | |
| | 90 | 9.7 | 1.4 | |
| 300 | 50 | 5.0 | 7.1 | 540 |
| | 70 | 2.4 | 2.6 | |
| | 90 | 1.7 | 1.0 | |
| | 140 | 1.8 | 1.2 | |
| 400 | 50 | 15.5 | 6.8 | 170 |
| | 70 | 15.0 | 20.2 | |
| | 90 | 30.6 | 52.8 | |
| | 140 | 41.0 | 74.6 | |
| 500 | 180 | 46.9 | 79.1 | |
| | 50 | 20.7 | 6.8 | 60 |
| | 70 | 15.9 | 4.7 | |
| | 90 | 17.7 | 5.9 | |
| | 140 | 25.2 | 7.0 | |
| | 180 | 26.7 | 8.0 | |
| 220 | 29.7 | 9.3 | | |

1 In the non-resonant case, this analysis sets limits on
2 coloron or stop-quark pair production, excluding 50-100
3 GeV/c^2 and 50-125 $/c^2$, respectively; see Table I and the
4 top of Fig. 5. The uncertainty on the theoretical cross-
5 section prediction comes from two sources summed in
6 quadrature. The first uncertainty is the envelope of the
7 PDF uncertainties from the CTEQ uncertainties and an
8 alternative PDF choice, MSTW2008LO [25] (5% relative).
9 The second uncertainty comes from a variation of the
10 renormalization and factorization scales by a factor of
11 two in each direction from their default values of the
12 per-event mass scale. These theoretical uncertainties are
13 illustrated in Figure 5.

14 In the resonant case, this analysis excludes axi-gluon
15 (A) production leading to pairs of σ particles and four-
16 gluon final state for $m_A \in [150, 400]$, $m_\sigma \in [50, m_A/2]$ in
17 the case of coupling to quarks $C_q = 0.4$ (see Table II and
18 the bottom of Fig. 5) which is close to the value required
19 to explain the top-quark A_{fb} result [9]. To be consistent
20 with this analysis, the couplings would have to be smaller

1 by an order of magnitude. Maintaining consistency with 38
 2 the top-quark A_{fb} result would require different couplings 39
 3 to light quarks and heavy quarks, with the heavy-quark 40
 4 coupling approaching the perturbative limit, $C_q < 1$. 41

5 We thank Martin Schmaltz, Gustavo Tavares, Can 42
 6 Kilic, Bogdan Dobrescu, Dirk Zerwas and Felix Yu for 43
 7 useful suggestions and technical advice. We thank the 44
 8 Fermilab staff and the technical staffs of the partici- 45
 9 pating institutions for their vital contributions. This 46
 10 work was supported by the U.S. Department of Energy 47
 11 and National Science Foundation; the Italian Istituto 48
 12 Nazionale di Fisica Nucleare; the Ministry of Education, 49
 13 Culture, Sports, Science and Technology of Japan; the 50
 14 Natural Sciences and Engineering Research Council of 51
 15 Canada; the National Science Council of the Republic 52
 16 of China; the Swiss National Science Foundation; the 53
 17 A.P. Sloan Foundation; the Bundesministerium für Bil- 54
 18 dung und Forschung, Germany; the Korean World Class 55
 19 University Program, the National Research Foundation 56
 20 of Korea; the Science and Technology Facilities Council 57
 21 and the Royal Society, UK; the Russian Foundation for 58
 22 Basic Research; the Ministerio de Ciencia e Innovación, 59
 23 and Programa Consolider-Ingenio 2010, Spain; the Slo- 60
 24 vak R&D Agency; the Academy of Finland; and the Aus- 61
 25 tralian Research Council (ARC). 62
 63
 64
 65
 66
 67
 68
 69

26 [1] T. Aaltonen *et al.* (CDF Collaboration), Phys. Rev. Lett. 70
 27 **101**, 202001 (2008). 71
 28 [2] V. M. Abazov *et al.* (D0 Collaboration), Phys. Rev. Lett. 72
 29 **100**, 142002 (2008). 73
 30 [3] T. Aaltonen *et al.* (CDF Collaboration), Phys. Rev. D 74
 31 **83**, 112003 (2011). 75
 32 [4] P. H. Frampton and S. L. Glashow, Phys. Lett. B **190**, 76
 33 157 (1987). 77
 34 [5] G. Marques Tavares and M. Schmaltz, Phys. Rev. D **84**, 78
 35 054008 (2011). 79
 36 [6] Y. Bai and B. A. Dobrescu, J. High Energy Phys. **07** 80
 37 (2011) 100. 81

[7] C. Kilic, T. Okui, and R. Sundrum, J. High Energy Phys. 07 (2008) 038; C. Kilic, S. Schumann, and M. Son, J. High Energy Phys. **04** (2009) 128.
 [8] S. P. Martin, In Kane, G.L. (ed.): *Perspectives on supersymmetry II* 1-153 (1997).
 [9] C. Gross, G. Marques Tavares, C. Spethmann, and M. Schmaltz, arXiv:1209.6375 [hep-ph] (2012).
 [10] G. Aad *et al.* (ATLAS Collaboration), Eur. Phys. J. C **71**, 1828 (2011).
 [11] T. Aaltonen *et al.* (CDF Collaboration), Phys. Rev. D **71**, 032001 (2005).
 [12] C. S. Hill, Nucl. Instrum. Methods A **530**, 1 (2004).
 [13] T. Aaltonen *et al.* (CDF Collaboration), Phys. Rev. D **45**, 001448 (1992).
 [14] CDF uses a cylindrical coordinate system with the z axis along the proton beam axis. For a particle or a jet, pseudorapidity is $\eta \equiv -\ln[\tan(\theta/2)]$, where θ is the polar angle relative to the proton beam direction, and ϕ is the azimuthal angle while transverse momentum $p_T = |p| \sin \theta$, and the transverse energy $E_T = E \sin \theta$.
 [15] A. Bhatti *et al.*, Nucl. Instrum. Methods A **566**, 375 (2006).
 [16] J. Alwall, P. Demin, S. de Visscher, R. Frederix, M. Herquet, F. Maltoni, T. Plehn, D. L. Rainwater, and T. Stelzer, J. High Energy Phys. **09** (2007) 028.
 [17] J. Pumplin *et al.* (CTEQ Collaboration), J. High. Energy Phys. **07** (2002) 012.
 [18] T. Sjostrand *et al.*, Comput. Phys. Commun. **238**, 135 (2001), version 6.422.
 [19] E. Gerchtein and M. Paulini, arXiv:physics/0306031 (2003).
 [20] M. L. Mangano, M. Moretti, F. Piccinini, R. Pittau, and A. D. Polosa, J. High Energy Phys. **07** (2003) 001.
 [21] T. Aaltonen *et al.* (CDF Collaboration), Phys. Rev. D **84**, 052010 (2011).
 [22] T. Aaltonen *et al.* (CDF Collaboration), Phys. Rev. D **73**, 032003 (2006).
 [23] A. Read, Nucl. Instrum. Methods A **425**, 357 (1999).
 [24] A. Read, J. Phys. G: Nucl. Part. Phys. **28**, 2693 (2002); T. Junk, Nucl. Instrum. Methods A **434**, 425 (1999).
 [25] A. D. Martin, W. J. Stirling, R. S. Thorne, and G. Watt, Eur. Phys. J. C **63**, 189 (2009).
 [26] W. Beenakker, M. Kramer, T. Plehn, M. Spira, and P. M. Zerwas, Nucl. Phys. **B515**, 3 (1998).